Internet-based experiment to measure the muon lifetime in real time

E. Ponce, M. Cid and C. Aguilar

Centro Interdisciplinario de Investigación y Enseñanza de la Ciencia and Facultad de Ciencias Físico Matemáticas, Benemérita Universidad Autónoma de Puebla, 72570 Puebla, Pue., México

H. Salazar and L. Villaseñor

Centro Interdisciplinario de Investigación y Enseñanza de la Ciencia, Benemérita Universidad Autónoma de Puebla, 72570 Puebla, Pue., México.

Received 25 February 2025; accepted 2 July 2025

We describe a web-based experiment to measure the lifetime of cosmic-ray muons that stop in a liquid scintillator detector. Our experimental setup consists of a container filled with liquid scintillator, a photomultiplier tube, a commercial electronics board (STEMlab 125-14) that includes an ARM-based computer with a field programmable gate array (FPGA) and an analog-to-digital converter (ADC). The muons we detect arrive at the detector as part of the secondary cosmic rays that are produced high in the Earth atmosphere when energetic primary cosmic rays collide with nitrogen and oxygen nuclei. The software we use to run this experiment in real time on the web uses Python code on the computer of the Red Pitaya board and HTML/Javascript code on the webpage. The experiment is located at the Centro Interdisciplinario de Investigación y Enseñanza de la Ciencia on the campus of the Benemérita Universidad Autónoma de Puebla (BUAP) in the city of Puebla, Mexico. We report a value for the effective mean lifetime of the stopping muons of $2.051 \pm 0.009\ \mu s$. This result is lower than the $2.197\ \mu s$ mean muon lifetime in vacuum due to the capture of negative muons by the nuclei of the atoms of the detector material. The experiment can be accessed through the webpage https://ciiec.buap.mx/Muon-Decay.

Keywords: Cosmic rays; muons; muon lifetime; muon capture; acquisition electronics.

DOI: https://doi.org/10.31349/RevMexFisE.23.010217

1. Introduction

The muon is a subatomic particle discovered in 1936 by Carl D. Anderson and Seth Neddermeyer [1]. They used a detector called cloud chamber that had been recently invented by Charles Wilson [2]; in fact, Wilson was awarded the Nobel Prize in Physics in 1927 for this invention. The muon has the same charge and spin as the electron and about 210 times more mass. Muons are produced by the collisions of primary cosmic rays with nuclei of nitrogen and oxygen at several kilometers above the Earth surface. These collisions take place through the strong interaction and produce other subatomic particles, dominated by pions and kaons, which eventually decay through the weak force into muons and neutrinos. Primary cosmic rays consist primarily of protons, those of low energies, up to about 100 MeVs, come from the Sun [3], while those of higher energies, up to about 1 PeVs [4], come from supernova in own galaxy and those with even higher energies, up to 100 EeVs, may come from active galactic nuclei (AGN) of distant galaxies [5,6]. Secondary cosmic rays were discovered in 1912 by Victor Hess [7], they consist of 4 components of particle showers: hadrons, muons, neutrinos and an electromagnetic component formed by electrons and gamma rays.

Energetic secondary muons produced at the top of the Earth atmosphere travel with speeds close to the speed of light. As explained below, their effective mean decay time when they decay in a non-vacuum medium may be slightly lower than τ_μ, however, their decay times may increase significantly due to the effect of time dilation, predicted by Albert Einstein in his Theory of Special Relativity in 1905. It is this time dilation that makes possible for a large number of muons to reach the Earth ground. The rate at which muons arrive at the ground at sea level is about 1 muon per square centimeter per minute [8] and increases to about 2 muons per square centimeter per minute for the 2000 m.a.s.l. altitude of Puebla City.

The rate of arrival of secondary muons to our detector is around 72 Hz, they arrive with a mean energy of around 3 GeV at sea level [9] so that most of them have enough energy to cross our detector. However, a small fraction of all the muons that reach our detector, about 0.8%, stop and decay inside the liquid scintillator that we use in our detector. We measure the time difference between the first pulse of scintillation light, which is due to the stopping muon, positive or negative, and the second pulse, due to the decaying positron or electron, respectively. By measuring the lifetime of a large number of these decaying muons, as explained in detail below, we measure the effective mean lifetime of the muons that decay inside our detector.

1.1. Decay of muons in vacuum

Muons are unstable subatomic particles; when an isolated muon is at rest in a vacuum medium, it decays with a mean lifetime denoted by τ_μ; this is a universal constant that has been measured with great precision and it has the following value $\tau_\mu = 2.1969811 \pm 0.0000022$ Pμs [10]. The mean

lifetime is the same for positive and negative muons, *i.e.*, the measured ratio τ_{μ^+} to τ_{μ^-} is 1.00002 ± 0.00008 [10]. For the purpose of this paper, we will use the measured value of the muon mean lifetime correct to 4 significant digits

$$\tau_\mu = 2.197 \quad \mu\text{s}. \tag{1}$$

Muons decay into electrons and neutrinos as illustrated below, depending on their electric charge

$$\boldsymbol{\mu^- \rightarrow e^- + \overline{v}_e + v_\mu}, \tag{2}$$

$$\boldsymbol{\mu^+ \rightarrow e^+ + v_e + \overline{v}_\mu}. \tag{3}$$

The muon mean lifetime τ_μ is related to another universal constant, Γ, which is the decay probability per unit time of a muon at rest, either positive or negative. Since this is an education paper, let's derive the formula for the probability that a muon at rest, which is known to exist at time $t = 0$, decays between time t and time $t + dt$, where dt is an infinitesimally small time interval. We will call this probability $P(t)dt$. Let's divide the time t into N intervals of size Δt, so that $t = N\Delta t$. The probability $P(t)\Delta t$ is equal to the joint probability that the muon does not decay in the first interval, which is $1 - \Gamma\Delta t$, times the probability that the muon does not decay in the second interval, which is also $1 - \Gamma\Delta t$, with a similar factor for the other intervals up to the N_{th} interval Δt. Finally, we multiply by the probability that the muon decays between time t and $t + dt$, which is Γdt.

We evaluate this probability in the limit in which $N \rightarrow \infty$ to obtain:

$$P(t)dt = \lim_{N\rightarrow\infty} (1 - \Gamma\Delta t)^N \Gamma dt, \tag{4}$$

substuting $\Delta t = t/N$ we obtain

$$P(t)dt = \lim_{N\rightarrow\infty} \left(1 - \frac{\Gamma t}{N}\right)^N \Gamma dt, \tag{5}$$

using the well known formula

$$e^x = \lim_{N\rightarrow\infty} \left(1 + \frac{x}{N}\right)^N, \tag{6}$$

we obtain

$$P(t)dt = \Gamma e^{-\Gamma t} dt. \tag{7}$$

Note that the probability density $P(t)$ satisfies the normalization condition:

$$\int_0^\infty P(t)dt = 1, \tag{8}$$

Now we can evaluate the mean decay time, also called mean lifetime, to obtain:

$$\langle t \rangle = \int_0^\infty P(t)tdt = \Gamma \int_0^\infty e^{-\Gamma t} t dt, \tag{9}$$

this integral can be evaluated by parts using $udv = d(uv) - vdu$ with $u = t$ and $dv = e^{-\Gamma t}tdt$. Therefore $v = -e^{-\Gamma t}/\Gamma$ and $du = dt$ with the result

$$\langle t \rangle = \tau_\mu = \frac{1}{\Gamma}, \tag{10}$$

with the mean muon lifetime given by Eq. (1).

1.2. Decay of positive muons in a medium

When negative muons traverse a non-vacuum medium, they interact with the molecules of that medium and gradually lose energy, some of the least energetic muons can stop in the medium and orbit the nuclei of the medium with non-relativistic velocities so that the time dilation is negligible.

Since nuclei are also positive, they repel the positive nuclei away from them, so that the orbital momentum of positive muons is different from zero. In this case the decay probability density of positive muons is the same as in vacuum as derived above, *i.e.*, the probability that the positive muon decays between time t and $t + dt$ is given by

$$P(t)dt = \Gamma e^{-\Gamma t} dt, \tag{11}$$

and their mean lifetime $\langle t \rangle$ is equal to $\tau_\mu = 2.197\mu$s.

1.3. Decay of negative muons in a medium

Negative muons that stop in a medium also orbit the nuclei of the atoms of the medium but in this case they are electrically attracted by the positive nuclei, so that they can have zero orbital momentum. In this case the negative muons can penetrate the nuclei and interact with the protons of the nucleus to produce neutrons, n, through the following muon capture reaction

$$\boldsymbol{\mu^- + p \rightarrow n + v_\mu}. \tag{12}$$

Next, we derive the formula for the probability that a negative muon that stops in a medium, which is known to exist at time $t = 0$, decays between time t and time $t + dt$, where dt is an infinitesimally small time interval. This derivation is similar to the previous one that led us to Eq. (7) We will call this probability $P(t)dt$.

In order to take into account the possible muon capture, we introduce the parameter Γ_c which is the rate of muon capture per unit time for our particular medium. Unlike Γ, which is a universal constant, Γ_c depends on the particular medium of our detector. Let's divide the time t into N intervals of size Δt, so that $t = N\Delta t$. The probability $P(t)\Delta t$ is equal to the joint probability that the muon does not decay and it is not captured in the first interval, which is $1 - (\Gamma + \Gamma_c)\Delta t$, times the probability that the muon does not decay and it is not captured in the second interval, which is also $1 - (\Gamma + \Gamma_c)\Delta t$, with similar factor for the other intervals up to the N_{th} interval Δt. Finally, we multiply by the probability that the

negative muon decays between time t and $t+dt$, which is Γdt.

We evaluate this probability in the limit in which $N \to \infty$ to obtain:

$$P(t)dt = \lim_{N\to\infty}(1-(\Gamma+\Gamma_c)\Delta t)^N \Gamma dt, \tag{13}$$

substuting $\Delta t = t/N$ we obtain

$$P(t)dt = \lim_{N\to\infty}\Big(1-\frac{(\Gamma+\Gamma_c)t}{N}\Big)^N \Gamma dt, \tag{14}$$

using Eq. 6 we obtain

$$P(t)dt = \Gamma e^{-(\Gamma+\Gamma_c)t}dt. \tag{15}$$

Note that the probability density $P(t)$ satisfies the normalization condition:

$$\int_0^\infty P(t)dt = \frac{\Gamma}{\Gamma+\Gamma_c}, \tag{16}$$

this is the total probability that the muon decays, it is different from zero because the muon can also be captured. Since we cannot detect the cases when the negative muon is captured with our experimental setup, we redefine a normalized probability density adapted for our restriction that we only observe negative muons that decay given by

$$P_{\text{norm}}(t)dt = (\Gamma+\Gamma_c)e^{-(\Gamma+\Gamma_c)t}dt, \tag{17}$$

that satisfies

$$\int_0^\infty P_{\text{norm}}(t)dt = 1. \tag{18}$$

Now we turn to the real case where we deal with both positive and negative muons.

1.4. Decay of positive and negative muons in a medium

In the secondary cosmic rays there are both positive and negative muons; therefore, positive and negative muons can stop in our detector medium. The decay probability density of a muon is given by the weighted sum of two terms, one for positive muons and the other for negative muons, where the first weight is the probability that the stopping muon is a positive muon, denoted by R, and the second weight is the probability that the stopping muon is a negative muon, denoted by $1-R$.

$$P(t)dt = \Gamma\Big(Re^{-\Gamma t} + (1-R)e^{-(\Gamma+\Gamma_c)t}\Big)dt. \tag{19}$$

This probability density is normalized to the total probability that the muon decays

$$\int_0^\infty P(t)dt = R + (1-R)\cdot\frac{\Gamma}{\Gamma+\Gamma_c}, \tag{20}$$

and the total probability that the negative muon is captured is

$$\int_0^\infty P_c(t)dt = (1-R)\cdot\frac{\Gamma_c}{\Gamma+\Gamma_c}, \tag{21}$$

and Eqs. (20) and (21) add up to 1.

As discussed in the previous section, we adapt the normalization of $P(t)$ given by Eq. (20) to 1 to take into account that we observe only events where the muons decay, *i.e.*, we do not observe the cases where the negative muons are captured. This normalized decay probability density is given by the ratio of Eqs. (19) and (20)

$$P_{\text{norm}}(t) = \frac{\Gamma\left(Re^{-\Gamma t} + (1-R)e^{-(\Gamma+\Gamma_c)t}\right)}{R+(1-R)\cdot\frac{\Gamma}{\Gamma+\Gamma_c}}, \tag{22}$$

where $\Gamma = 1/\tau_\mu$ is the decay rate of muons, either positive or negative, per unit time and Γ_c is the rate of capture of negative muons per unit time for the medium where muons stop in our experimental setup, *i.e.*, liquid scintillator.

The mean decay time of this probability density is

$$\langle t\rangle = \int_0^\infty t\, P_{\text{norm}}(t)\, dt = \frac{R\cdot\frac{1}{\Gamma}+(1-R)\cdot\frac{\Gamma}{(\Gamma+\Gamma_c)^2}}{R+(1-R)\cdot\frac{\Gamma}{\Gamma+\Gamma_c}}, \tag{23}$$

note that this mean decay time, $\langle t\rangle$, reduces to τ_μ when $R=1$, *i.e.*, we have only positive muons, or $\Gamma_c = 0$. *i.e.*, we are in vacuum where negative muons are not captured.

We can approximate Eq. (22) by a single exponential

$$P_{\text{eff}}(t) = \Gamma_{\text{eff}}\, e^{-\Gamma_{\text{eff}}t} = \Gamma_{\text{eff}} e^{-\frac{t}{\tau_{\text{eff}}}}, \tag{24}$$

which has a mean decay time

$$\langle t\rangle = \tau_{\text{eff}} = \frac{1}{\Gamma_{\text{eff}}}, \tag{25}$$

by requiring that both $P_{\text{eff}}(t)$ and $P_{\text{norm}}(t)$ have the same mean decay time, *i.e.*, such that Eq. (23) and (25) are equal

$$\tau_{\text{eff}} = \frac{R\cdot\frac{1}{\Gamma}+(1-R)\cdot\frac{\Gamma}{(\Gamma+\Gamma_c)^2}}{R+(1-R)\cdot\frac{\Gamma}{\Gamma+\Gamma_c}}, \tag{26}$$

which simplifies to

$$\tau_{\text{eff}} = \tau_\mu\cdot\frac{R+(1-R)\cdot\frac{1}{(1+\gamma)^2}}{R+(1-R)\cdot\frac{1}{1+\gamma}}, \tag{27}$$

where $\gamma = \Gamma_c/\Gamma = \Gamma_c\cdot\tau_\mu$ is the relative capture rate of negative muons and τ_μ is the mean muon lifetime given by Eq. (1).

In this experiment we measure this effective mean decay time, which we denote by τ_{eff} in the rest of this paper. Note that when muons decay in a medium τ_{eff} is lower than the muon mean lifetime τ_μ. In Sec. 5, we discuss the possibility to use this same experiment to perform a fit of the experimental data to Eq. (22) to measure the mean muon lifetime, τ_μ, the ratio of positive to negative muons, $R/(1-R)$ and the rate of capture of negative muons per unit time, Γ_c.

1.5. Advantages of internet-based experiments

This experiment constitutes an excellent tool to introduce and motivate students to learn the fields of nuclear physics and high-energy physics. It includes the construction of a simple detector, the use of simple data acquisition code written in `Python`, the use of code written in `Verilog` [11] to program the field programmable gate array (FPGA) [12], the use of analysis techniques to fit the data to a model and finally, the web-based character of this experiment, requires the use of modern software tools to display the experiment on a webpage using `HTML`, `PHP` and `Javascript`.

The main advantage of internet-based experiments is that they can be handled by much wider groups of students, docents and general public from all over the world, optimizing the human and physical resources required for their implementation.

The goal of this experiment is to detect, digitize and measure the time interval between any two consecutive pulses detected in a time window of 20 μs by the experimental setup. The first pulse is produced, most of the time, by an incoming muon of low energy, and the second pulse is due, most of the time, to an outgoing positron or electron of that incoming muon once it stops and decays inside the detector volume. These pulses are created by the photomultiplier tube (PMT) when it receives light produced by the interaction of the charged particles moving inside the detector that gradually loose energy by ionization of the molecules of the scintillating liquid. These types of events constitute our signal in this experiment.

Occasionally, the second pulse can be produced by a second muon reaching the detector within the short time window of 20 μs after a first muon also crosses the detector. These double-coincidence events constitute the background noise for this experiment. The window of 20 μs is chosen as a compromise to collect enough numbers of both, signal events, where the muons decay with an effective mean time of around 2 μs, and background noise events, due to accidental crossing of a second muon after a first muon crosses the detector medium.

It is important to collect enough statistics of these two types of events to make good estimations of both, the effective mean decay time and the constant background, as modeled through Eq. (28) in Sec. 3. The use of a different time window, selected around 20 μs, should not affect the measurement of the central value of the effective mean lifetime, although it may have an effect on the uncertainty of the measurement.

In the next sections we describe the experimental setup, the data acquisition software and the data analysis that we perform to measure the effective mean lifetime of the stopping muons and other properties of the first and second pulses.

FIGURE 1. Photo of the detector at the moment of assembly. The liquid scintillator and the PMT are clearly visible. The PMT is the model Electron Tubes 9354KB with a diameter of 200 mm. The cylindrical steel container has a diameter of 52 cm and it is filled with liquid scintillator up to a height of 45 cm.

2. Experimental setup

2.1. Detector

The detector we use consists of a 95-liter steel container filled with liquid scintillator (BC-503) coupled to a fast photomultiplier tube (PMT), Electron Tubes 9354KB. The diameter of the PMT is 200 mm. The cylindrical steel container has a diameter of 52 cm and it is filled with liquid scintillator up to a height of 45 cm, as shown in Fig. 1.

The scintillation light produced by the interaction of the muons and electrons with the detector media is amplified by the PMT which is located on top of the liquid scintillator, inside the container. The PMT surface is slightly immersed into the liquid to ensure optimal collection of the scintillation light. The container is light-tight to prevent spurious pulses due to ambient light that might reach the PMT.

The optimum operating voltage of the PMT is 1000 V. This value was selected by finding the plateau of the single-pulse rate in such a way that small variations of the high-voltage power supply of the PMT lead to small variations in the single-pulse rate, which is around 90 Hz.

Figure 2 shows a photo of the STEMlab 125-14 electronics board, also known as Red Pitaya board. It includes a computer with a two-core ARM processor, a FPGA (ZYNQ 7010), two fast analog-to-digital converter (ADCs) inputs and two fast digital-to-analog converter (DACs) outputs, each with a maximum sampling rate of 125 MHz. Therefore, we can digitize the PMT signals with a time resolution of 8 ns. For this experiment we use only one of the ADC inputs and we do not use the DAC outputs. As described below, we modified the FPGA standard code of the Red Pitaya board to trigger the pulse acquisition when two PMT pulses occur in a time window of 20 μs.

Variations in atmospheric pressure lead to small variations in single-particle rates in our experimental setup. Variations in temperature of the data-acquisition (DAQ) hardware also lead to small variations in the single-particle rates. However, neither of these variations leads to significant changes

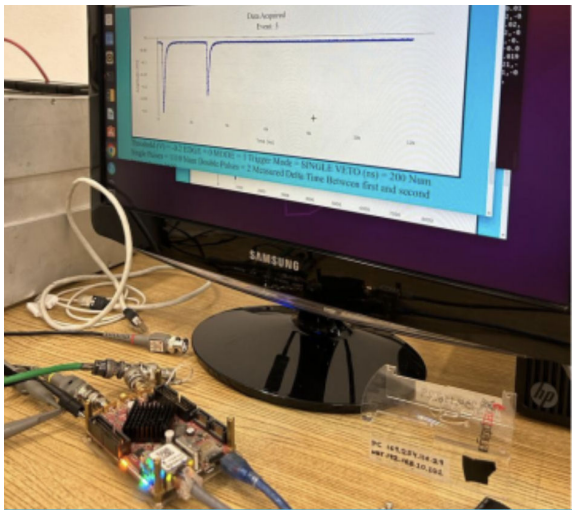

FIGURE 2. Picture of the Red Pitaya board and a computer that displays one event. The computer that controls the experiment is the two-core ARM processor of the ZYNQ 7010 chip located on the Red Pitaya board displayed on the bottom left corner of the image.

in the rates of double-pulses. These variations do not change the decay times of muons either.

The Red Pitaya board represents an economical way of digitizing the PMT pulses compared to other options that may require more expensive equipment. However, we needed to reprogram the FPGA of the Red Pitaya board to detect double pulses, known as trigger signal, and to digitize the PMT pulses within the 20 μs time window after the detection of the first PMT pulse. We describe the software for reprogramming the FPGA of the Red Pitaya board and the data acquisition software in the next section.

2.2. Software

2.2.1. Firmware of the field programmable gate array

The FPGA contained on the Red Pitaya board is the Xilinx ZYNQ 7010 [13]. The code to control this FPGA for the purpose of detecting two consecutive PMT pulses above a given threshold and digitizing them using one of the two 14-bit ADCs was written using the hardware description language (HDL) named Verilog. The binary code that constitutes the firmware of the ZYNQ FPGA was created with the Vivado Design Suite which is a free software suite for synthesis and implementation of HDL [14,15].

Once the data with the digitized PMT pulses is collected on the Red Pitaya board, it is transferred to the web server by a program written in Python that controls the data acquisition process as explained in the next subsection.

2.2.2. Data acquisition software

We use a `Python` script running on the ZYNQ chip on the Red Pitaya board under the `Ubuntu` operating system to control the experiment and to acquire the data. The `Python` script checks when there is a double-pulse trigger above the threshold selected and reads the digitized PMT pulses stored on the ZYNQ 70010 FPGA into the computer on the Red Pitaya board. The threshold is chosen as 5 mV to allow for a clear differentiation between real PMT pulses and fluctuations on the PMT baseline. The reader can use the webpage to experiment with different amplitude thresholds on the first and the second pulses to check that the effective mean lifetime of the stopping muons is independent of this threshold, although higher thresholds than the 5 mV used in the previous analysis will increase the statistical error as they may decrease the number of events that pass the threshold cut.

Upon the occurrence of a double-pulse trigger, the acquisition code reads the data from the ADC that digitizes the PMT signal with a sampling rate of 125 MS/s, *i.e.*, with a time resolution of 8 ns. Each event collected by the DAQ system is arranged as a row that includes a header with the most relevant information about the data acquisition parameters followed by the data points in comma-separated value (CSV) format.

Upon acquisition, each event is compressed and sent through an HTTP request to a server where it is stored and distributed over internet through the webpage of the experiment using `HTML`, `PHP` and `Javascript` [16]. As mentioned earlier, the webpage of the experiment is https://ciiec.buap.mx/Muon-Decay.

3. Data analysis

In this section we describe the analysis we perform on the collected data. Firstly, we make a histogram of the measured time difference between the arrival time of the first and second PMT pulses. We take the number of bins in our histogram equal to 100 and we use only events that have a time difference between the first and the second pulse between 0 and 20 μs, *i.e.*, the bin size is 200 ns.

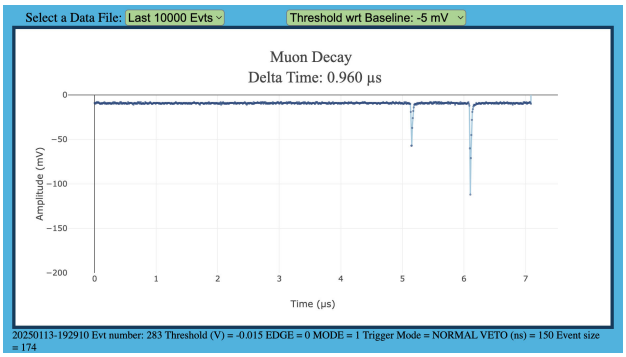

FIGURE 3. One event showing the first and the second PMT pulses as digitized with the Red Pitaya board with a time resolution of 8 ns. The amplitude of the baseline is 9.5 mV and the threshold selected on the DAQ script was -15 mV. The difference in arrival times between the two PMT pulses is 0.960 μs. The event header is printed beneath the plot.

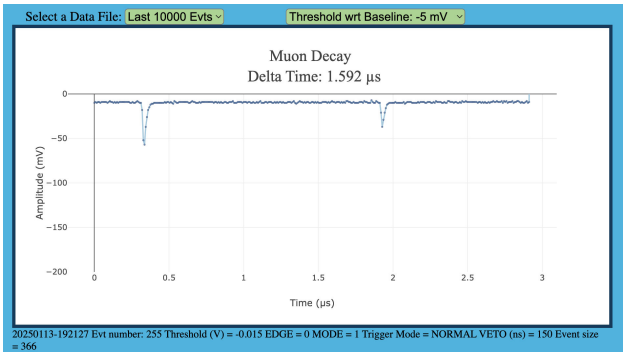

FIGURE 4. Another double-pulse event showing the first and the second PMT pulses as digitized with the Red Pitaya board. The amplitude of the baseline is 9.5 mV and the threshold selected on the DAQ script was -15 mV. The difference in arrival times between the two PMT pulses is 1.592 μs. The event header is printed beneath the plot.

According to our analysis of Sec. 1.4, we approximate the distribution of these time differences by an effective single-exponential distribution, given by Eq. (24), plus a constant term to take into account the background noise events, given by the following equation:

$$N(t) = Ae^{-t/\tau_{\text{eff}}} + B, \tag{28}$$

where $N(t)\Delta t$ is the number of events where the second pulse arrives between t and $t + \Delta t$, τ_{eff} is the muon effective mean lifetime, A and B are constant parameters. τ_μ, A and B are measured by the fit procedure.

As mentioned above, occasionally the second PMT pulse is produced by a second muon reaching the detector within the active window of 20 μs started for every detection of a first PMT pulse. These double-pulse muon coincidences constitute the background noise for our measurement of the muon effective mean lifetime. The parameter B represents this background noise per bin and we assume that it is constant, given that its distribution is also exponential but with a characteristic decay time of the order of the inverse of the frequency of single PMT pulses, which is near 90 Hz. Therefore, the number of background events per bin is flat at the scale of 20 μs and B is constant.

Next, we use two different ways of doing the fit of the data to the exponential model, given by Eq. (28). Firstly, a gradient descent method and, secondly, a linear least squares regression method. In both cases we evaluate the quality of the fit through the value of the mean squared error (MSE) given as follows:

$$\text{MSE} = \frac{1}{N - bin_0} \sum_{i=bin_0}^{N} \left(y_i - \hat{y}_i\right)^2, \tag{29}$$

where bin_0 is the initial bin and N is the total number of bins in the histogram, *i.e.*, $N = 200$, y_i is the measured data in the i-th bin, $\hat{y}_i$ is the predicted value for the i-th bin, $(y_i - \hat{y}_i)^2$ is the squared difference between actual and predicted values of the i-th bin.

The webpage offers the option of performing these two fitting procedures, where the user can select the amplitude threshold of both PMT pulses and the first bin to include in the fit, with each bin having a width of 200 ns. The amplitude thresholds can be selected among the values -5 mV, -10 mV, -15 mV, -20 mV and -30 mV, with respect to the baseline of the PMT signal digitized by the fast ADC.

Alternatively, the user can download the last 10000 double-pulse events from the webpage of the experiment to perform her or his own data analysis. These events are contained in the file named MD10000Last.csv which is updated automatically every time the DAQ systems acquires 10000 events. The user has the option to perform a fit on a larger number of events by merging several of these files.

In case the user decides to perform a fit on a merged file with several thousands of events, he or she can use the Python script provided on the webpage to read the events and she or he can add additional code to extract the time difference between the first and the second pulses for a given threshold, as well as other relevant parameters of the events, as discussed below.

The general objective of the two fit methods described is to minimize Eq. (29) by using different procedures as discussed in detail in the following subsections.

3.1. Fit using gradient descent

We can substitute Eq. (28), using τ instead of τ_{eff} for simplicity, in Eq. (29) to obtain:

$$\text{MSE} = \frac{1}{N - bin_0} \sum_{i=bin_0}^{N} \left(y_i - \left(Ae^{-\frac{t_i}{\tau}} + B\right)\right)^2. \tag{30}$$

The gradient descent method minimizes the value of Eq. (30) by adjusting A, τ, and B in an iterative way by using the general technique of gradient descent [17]. This technique uses the gradient of Eq. (30) through the calculation of its partial derivatives with respect to each parameter:

$$\frac{\partial \text{MSE}}{\partial A} = -\frac{2}{N - bin_0} \times \sum_{i=bin_0}^{N} \left(y_i - \left(Ae^{-\frac{t_i}{\tau}} + C\right)\right) e^{-\frac{t_i}{\tau}}, \tag{31}$$

$$\frac{\partial \text{MSE}}{\partial \tau} = \frac{2}{N - bin_0} \times \sum_{i=bin_0}^{N} \left(y_i - \left(Ae^{-\frac{t_i}{\tau}} + C\right)\right) \cdot Ae^{-\frac{t_i}{\tau}} \cdot \frac{t_i}{\tau^2}, \tag{32}$$

$$\frac{\partial \text{MSE}}{\partial B} = -\frac{2}{N - bin_0} \sum_{i=bin_0}^{N} \left(y_i - \left(Ae^{-\frac{t_i}{\tau}} + C\right)\right), \tag{33}$$

to update each parameter iteratively:

$$\theta^{(t+1)} = \theta^{(t)} - \eta \frac{\partial \text{MSE}}{\partial \theta}, \tag{34}$$

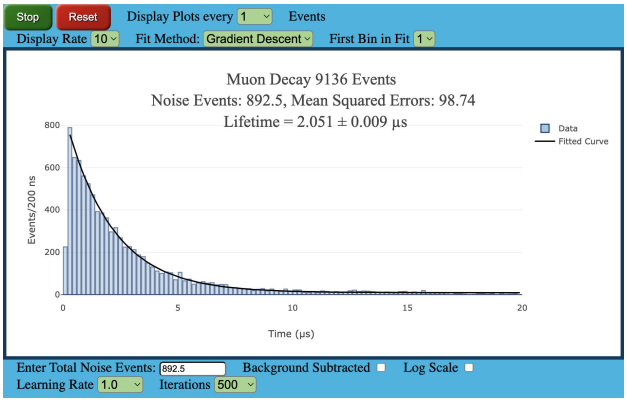

FIGURE 5. Illustration of the fit of the model described in Eq. (28) using the gradient descent method. The number of iterations used was 500 with a learning rate of 1.0. The total number of background events measured was 892.5 events out of a total of 9136 events, *i.e.*, the background noise represents about 9.8% of the data. The measured effective mean lifetime is 2.051 ± 0.009 μs. The mean squared error (MSE) of the fit was 98.74.

where θ is one of A, τ, or B. η is the parameter that controls the step size, usually called the *learning rate* and $\partial \text{MSE}/\partial\theta$ is the θ component of the gradient of the mean squared error.

We start with initial values chosen arbitrarily, but close to the expected values, for the three parameters. Next we repeat the iteration given by Eq. (34) for a fixed number of iterations with a given *learning rate*, where the number of iterations, the *learning rate* and the initial bin, bin_0, can be selected on the webpage.

The standard error in the decay parameter τ can be estimated using the curvature of the loss function at its minimum. This method is based on the second derivative of the likelihood (or equivalently, the cost function) and is discussed in the context of particle physics in *Statistics for Nuclear and Particle Physicists* by Lyons [18].

See *e.g.*, [19], Chapter 5, for methods on parameter estimation and error propagation using the curvature of the likelihood or chi-squared surface.

Once we obtain the optimal value of the decay constant τ by minimizing the mean squared error (MSE), we estimate its uncertainty using the curvature of the loss function [18]. This method is based on the second derivative of the loss with respect to τ and provides an approximation to the standard error of τ.

We consider the model function:

$$f(t; A, \tau, B) = A\, e^{-t/\tau} + B, \tag{35}$$

and the mean squared error:

$$\text{MSE}(\tau) = \frac{1}{N} \sum_{i=1}^{N} \left(y_i - f(t_i; A, \tau, B)\right)^2 . \tag{36}$$

Near the minimum of the MSE, the curvature of the loss function with respect to τ determines the uncertainty in its value. The standard error in τ can be approximated as:

$$\sigma_\tau = \sqrt{\frac{2 \cdot \text{MSE}}{\frac{\partial^2 \text{MSE}}{\partial \tau^2}}}. \tag{37}$$

We estimate the second derivative numerically using finite differences:

$$\frac{\partial^2 \text{MSE}}{\partial \tau^2} \approx \frac{\text{MSE}(\tau + \delta) - 2\,\text{MSE}(\tau) + \text{MSE}(\tau - \delta)}{\delta^2}, \tag{38}$$

where δ is a small step (*e.g.*, 10^{-4}) around the optimal value of τ.

This approach assumes that the loss function is approximately quadratic near the minimum, and the noise is approximately Gaussian. These approximations are valid in our high-statistics experiment.

3.2. Fit using linear least squares regression

The method of linear least squares regression [20] can be applied to fit an exponential function of the form:

$$\hat{y}_i = A e^{-\frac{t_i}{\tau_{\text{eff}}}} + B_i, \tag{39}$$

to the data where $\hat{y}_i$ is the value of the fit for bin_i, t_i is the time for bin_i, τ_{eff} is the fitted effective mean lifetime, A is the fitted amplitude and B_i is the constant number of background events per bin, *i.e.*, $B_i = B/N$ with B the total number of background events and N the number of bins.

Since we do not know the value of the total background events, B, we can repeat this procedure for various values of B and use the fitted parameters of A and τ that produce the minimum value of the MSE given by Eq. (29).

Next we linearize Eq. (39) by taking the natural logarithm to obtain:

$$\ln(\hat{y}_i - B_i) = \ln(A) - \frac{t_i}{\tau_{\text{eff}}} = D + \beta t_i, \tag{40}$$

where $D = \ln(A)$ and $\beta = -1/\tau_{\text{eff}}$.

This procedure transforms the fit to a linear regression problem in which the parameters β and D are easily estimated by minimizing the sum of squared residuals:

$$\text{SSE} = \sum_{i=bin_0}^{N} \left[\ln(y_i - B_i) - (D + \beta t_i)\right]^2, \tag{41}$$

where y_i is the number of events in bin_i.

The solution leads to the following values for β and D [20]:

$$\beta = \frac{\sum_{i=bin_0}^{N} (t_i - \bar{t})(z_i - \bar{z})}{\sum_{i=bin_0}^{N} (t_i - \bar{t})^2}, \tag{42}$$

and

$$D = \bar{z} - \beta \bar{t}, \tag{43}$$

where:

$$\bar{t} = \frac{1}{N - bin_0} \sum_{i=bin_0}^{N} t_i, \tag{44}$$

is the mean of the time values, and

$$\bar{z} = \frac{1}{N - bin_0} \sum_{i=bin_0}^{N} \ln(y_i - B_i), \tag{45}$$

is the mean of the natural logarithm of the observed values with the background per bin subtracted.

The standard deviation on β is

$$\sigma_\beta^2 = \frac{1}{n\sum t_i^2 - (\sum t_i)^2} \cdot \sum (y_i - D - \beta t_i)^2, \tag{46}$$

and the standard deviation on τ_{eff} is

$$\sigma_\tau = \left| \frac{d\tau}{d\beta} \right| \cdot \sigma_\beta = \frac{1}{\beta^2} \cdot \sigma_\beta. \tag{47}$$

Next, we recover A and τ_{eff} using:

$$A = e^D, \tag{48}$$

and

$$\tau_{\text{eff}} = -\frac{1}{\beta}. \tag{49}$$

Note that, unlike the case of the gradient descent method, this approach can only use data bins of the histogram for which $\ln(y_i - B_i) > 0$, *i.e.*, it uses fewer data points and therefore its statistical errors are expected to be larger than the fitted errors using gradient descent. Another reason for preferring the gradient descent method is that the logarithmic transformation in Eq. (40) distorts the Gaussian nature of the statistical uncertainties, especially in bins with low counts, and may underestimate or overestimate the associated uncertainty on the effective mean lifetime.

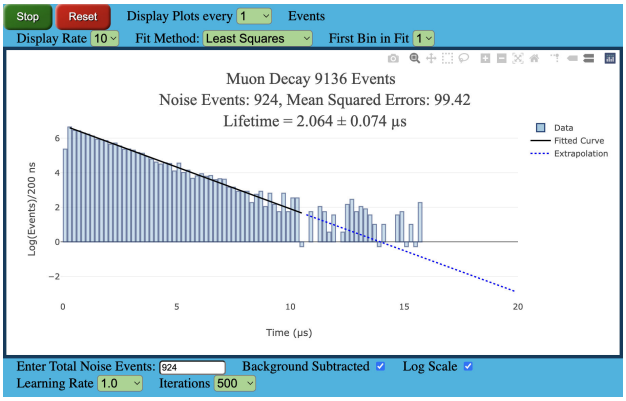

FIGURE 6. Result of a linear least squares regression on a file of 9136 events. This is a two-parameter fit to the model given in Eq. (39) with the total number of background events adjusted to minimize the mean squared error (MSE); the total background that minimized the mean squared error in this case was 924 events, *i.e.*, about 10% of the total data. The measured effective mean lifetime is τ = 2.064 $\pm$ 0.074 μs. This number is consistent with $\tau_{\text{eff}} = 2.051 \pm 0.009$ μs obtained with the gradient descent method shown in Fig. 5.

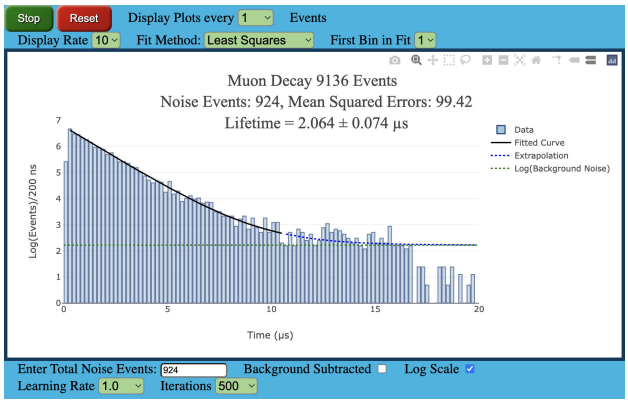

FIGURE 7. The same fit as in Fig. 6 is also displayed in logarithmic scale with the total background of 924 events not subtracted.

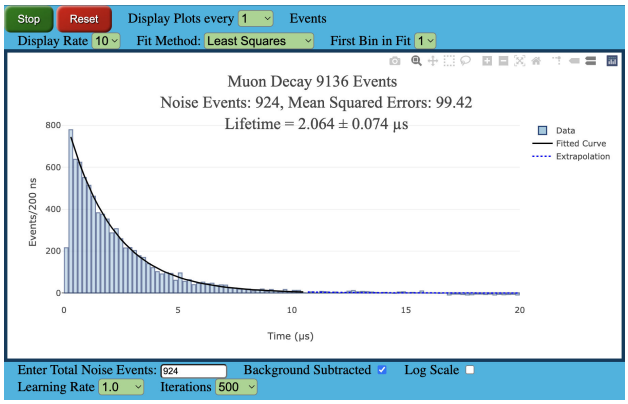

FIGURE 8. Same fit as in Fig. 6 but displayed in linear scale with the total background of 924 events subtracted.

The webpage provides the option of displaying the fitting plot with or without background subtraction and in linear or logarithm scale. It also provides the option of using any test value for the total number of background events and also the selection of the initial bin b_0. The reader is encouraged to estimate the effective mean lifetime of the muons that decay in the liquid scintillator by using other methods and comparing the results with the gradient descent method.

4. Discussion and results

The main result that this web-based experiment produces is the measurement of the muon effective mean lifetime for muons that stop in the liquid scintillator. As mentioned earlier, this value is the average of the measured decay times of positive and negative muons. However, positive muons have the same mean lifetime in a medium and in vacuum, *i.e.*, $\tau_\mu = 2.197$ μs, whereas negative muons have a shorter mean decay time when they stop in a medium due to the fact

that in addition to decaying they can be captured by protons, as mentioned earlier, through the following process:

$$\boldsymbol{\mu^- + p \rightarrow n + \nu_\mu}, \tag{50}$$

resulting in the production of a neutron and a neutrino, and sometimes a gamma photon, for each muon-capture event.

Other important results that can be obtained with this experiment are the measurement of the charge ratio of secondary cosmic-ray muons, and the measurement of the Michel parameter related to the energy spectrum of the positrons or electrons resulting from the decay of the positive or negative muons, respectively. These possible measurements are discussed below.

4.1. Measurement of the muon effective mean lifetime

Figure 5 shows the result of the gradient descent fit to a data set of 9136 events with the amplitudes of the first and second PMT pulses above 5 mV, with respect to the baseline. The value obtained for the effective mean lifetime of the stopping muons is

$$\tau_{\text{eff}} = 2.051 \pm 0.009 \ \mu\text{s}, \tag{51}$$

with MSE = 98.74.

Likewise, Fig. 6 shows the result of the linear least squares regression. The total number of background events that minimizes the mean squared error, MSE, given by Eq. (29) in this case is 924. The value obtained for the effective mean lifetime is

$$\tau_{\text{eff}} = 2.064 \pm 0.074 \ \mu\text{s}, \tag{52}$$

with a mean squared error of 99.42.

These two values are in agreement, within the errors shown. However, since the gradient descent method produces the fit with the smallest mean squared error and it also evaluates the background noise automatically, we refer to the measured value of the effective mean lifetime with the gradient descent analysis, see Eq. (53), as the most accurate measurement that this experiment produces for the effective mean lifetime of the stopping muons, in fact, the measured statistical error using the gradient descent method is also the smallest of the two methods, being about 0.4%. This is partly due to the fact that the fit with the gradient descent method uses all the data points, whereas the linear least squares regression uses less than the total number of data events, as discussed above. The reader can use the webpage to experiment with different amplitude thresholds on the first and the second pulses to check that the effective mean lifetime of the stopping muons is independent of this threshold, although higher thresholds than the 5 mV used in the previous analysis will increase the statistical error as they decrease the number of events.

The reader can reduce this statistical error substantially by merging several files with 10000 events by downloading them from the webpage over several days of operation of the experiment.

The fact that the value measured for the effective mean lifetime of the stopping muons is lower than 2.197 μs is related to what we discussed in Sec. 1.4 that we are measuring the effective mean lifetime in a medium where negative muons can be captured. The effective mean lifetime that we measure, τ_{eff}, is related to the ratio of positive to negative muons, $R/1-R$, the mean muon lifetime, τ_μ and the rate of capture of negative muons per unit time, Γ_c, according to Eq. (27). This relationship leads to a possible direct measurement of these parameters as discussed in the next subsection.

4.2. Measurement of the charge ratio secondary cosmic-ray muons

This experiment is quite simple and therefore one would not expect that the charge ratio of secondary cosmic-ray muons could be measured with it. However, by using the fact that negative muons that stop in the detector can orbit the nuclei with zero angular momentum, unlike positive muons that are repelled electrically by atomic nuclei, the measured lifetime of negative muons has a slightly steeper decay time distribution than for positive muons. This fact can be used to measure the ratio of the number of positive to negative atmospheric muons reaching the Earth's surface. Therefore, we can use this same experiment to collect much more data to perform a fit of the experimental data to Eq. (22), with the purpose of making direct measurements of the ratio of positive to negative muons in the secondary cosmic rays, $R/(1-R)$, the mean muon lifetime, τ_μ, and the relative capture rate of negative muons in the liquid scintillator, $\gamma = \Gamma_c \cdot \tau_\mu$, see [21] where this was achieved using an experimental setup using a simpler data acquisition system.

4.3. Measurement of the Michel distribution

The positron and electron energy spectrum in the decay of positive and negative muons, respectively, permits to test the V-A structure of the charged weak current. More advanced

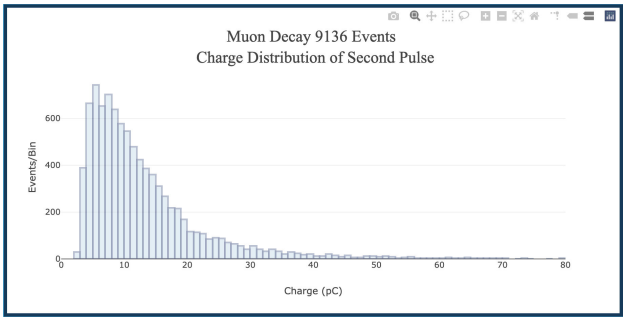

FIGURE 9. Charge distribution of the second PMT pulse as digitized by the fast ADC of the Red Pitaya board with a time granularity of 8 ns and a threshold of 5 mV with respect to the baseline. This plot is the basis to obtain the Michel parameter related to the energy spectrum of the positrons and electrons resulting from the decaying muons. The charge is measured in pC.

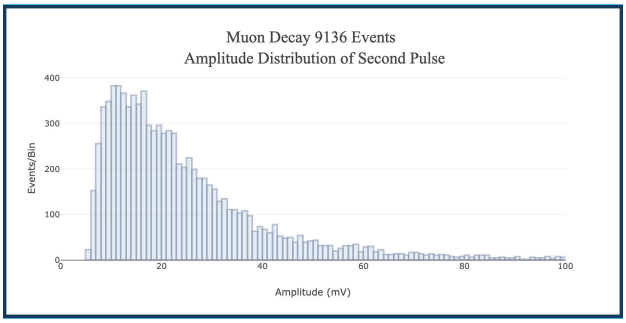

FIGURE 10. Amplitude distribution of the second PMT pulse as digitized by the fast ADC of the Red Pitaya board with a time granularity of 8 ns and a threshold of 5 mV with respect to the 9.5 mV baseline. The amplitude is measured in mV with respect to the baseline.

users can compare the simulated energy spectrum that includes the geometry of the detector and the time response of the PMT with the measured distribution of the integrated charge of the second PMT pulse, shown in Fig. 9. The analysis of this measurement requires a detailed simulation of the signal produced by the decay electrons and positrons on the detector. Figure 10 shows the distribution of the amplitude of the second pulse, which must also be compared with the simulations. A standard tool to perform this simulation is the software package named GEANT4 which is a free toolkit for the simulation of the passage of particles through matter [22].

4.4. Measurement of additional properties of the first and second pulses

In addition to the measurement of the effective mean lifetime of the stopping muons, the webpage plots the distributions of the charge, see Fig. 11, and amplitude, shown in Fig. 12, of the first pulse. In addition, the webpage also includes scatter plots of the amplitudes of the first and second pulses as a function of their difference in arrival times.

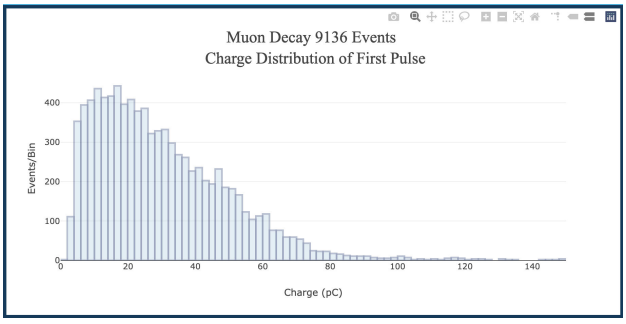

FIGURE 11. Charge distribution of the first PMT pulse as digitized by the fast ADC of the Red Pitaya board with a time granularity of 8 ns and a threshold of 5 mV with respect to the baseline. The charge is measured in pC.

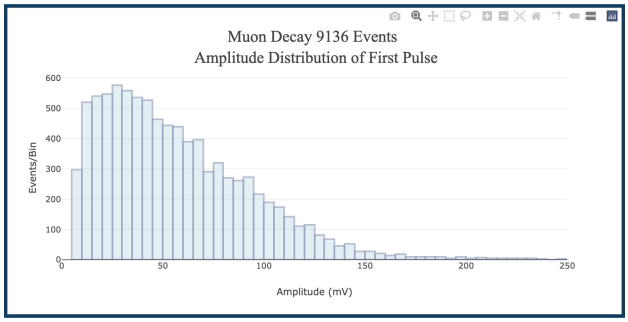

FIGURE 12. Amplitude distribution of the first PMT pulse as digitized by the fast ADC of the Red Pitaya board with a time granularity of 8 ns and a threshold of 5 mV with respect to the 9.5 mV baseline. The amplitude is measured in mV with respect to the baseline.

5. Conclusions

We have described an internet-based experiment to measure the effective mean lifetime of muons in real time. This experiment uses a liquid scintillator detector, a photomultiplier tube, a commercial electronics board known as Red Pitaya board, that includes an ARM-based computer with a field programmable gate array (FPGA) and a fast analog-to-digital converter (ADC). The muons we detect arrive at the detector as part of the secondary cosmic rays that are produced when energetic primary cosmic rays collide with nitrogen and oxygen nuclei high in the Earth atmosphere. The software we use to run this experiment in real time on the internet uses `Python` code on the computer of the Red Pitaya board and `HTML`, `PHP` and `Javascript` code on a web server located at the Centro Interdisciplinario de Investigación y Enseñanza de la Ciencia (CIIEC) at the Benemérita Universidad Autónoma de Puebla (BUAP) in the city of Puebla, Mexico.

We have illustrated the fitting process of the experimental data to the model given by Eq. (28) by using two methods, the first method based on the minimization of the mean squared error using gradient descent, and a least squares method as the second method. The least squares method offers a simpler and more intuitive approach. It has the advantage of yielding an analytical solution, which makes it computationally efficient and easy to implement without iterative procedures. This can be particularly useful for quick estimates or educational purposes where the limitations of the method are acceptable. Additionally, when the bin counts are sufficiently large and statistical fluctuations are small, the method can provide a reasonably good approximation of the decay constant τ_{eff}.

In contrast, using the second method, *i.e.*, fitting the model by minimizing the Mean Squared Error (MSE) using gradient descent, is more robust and statistically appropriate. This method directly compares the model to the original (untransformed) data and allows for a flexible treatment of nonlinear models, such as exponential decay plus background.

Unlike the logarithmic linearization method, gradient descent does not assume Gaussian-distributed errors in log space and can properly handle bins with low or zero counts. As such, it provides a more accurate estimation of the decay parameter τ_{eff} and its uncertainty when combined with curvature-based error analysis.

The webpage of the experiment includes two fitting methods to extract the value of the effective mean lifetime of the muons that stop in our detector. The most accurate result is obtained with a gradient descent fit of the data to an exponential model resulting in the following value:

$$\tau_{\text{eff}} = 2.051 \pm 0.009 \ \mu\text{s}, \tag{53}$$

with a mean squared error (MSE) equal to 98.74. The uncertainty on τ_{eff} is only the statistical error. This error can be substantially reduced by merging several files with 10000 events each that can be downloaded from the webpage of the experiment over several days of operation. The use of the linear least squares regression provides consistent results with the previous value of the muon effective mean lifetime.

Besides the effective mean lifetime of the muons, this experiment has the potential to measure the charge ratio of secondary muons that reach the detector. In addition, this experiment may also be used to study the energy spectrum of the decay electrons and positrons.

The experiment can be accessed freely through the webpage https://ciiec.buap.mx/Muon-Decay. We will try to keep the experiment running most of the time on a 7/24 basis, except for brief periods of improvements and maintenance[i].

---

i. You can send an email to epifanio.ponce@correo.buap.mx to inquire about the resumption of the experiment in case the experiment, or the webpage, is down for maintenance or another reason.

1. C. D. Anderson and S. H. Neddermeyer, Cloud Chamber Observations of Cosmic Rays at 4300 Meters Elevation and Near Sea-Level, *Phys. Rev.* **50** (1936) 263, https://doi.org/10.1103/PhysRev.50.263
2. N. N. Das Gupta and S. K. Ghosh, A Report on the Wilson Cloud Chamber and its Applications in Physics, *Rev. Mod. Phys.* **18** (1946) 225-365, https://doi.org/10.1103/RevModPhys.18.225
3. T. Sloan and A. W. Wolfendale, Cosmic rays, solar activity and the climate, *Environ. Res. Let.* **8** (2013) 045022, https://doi.org/10.1088/1748-9326/8/4/045022
4. P. Carlson, A century of cosmic rays, *Phys. Today* **65** (2012) 30, https://doi.org/10.1063/PT.3.1437
5. R. A. Batista, The Quest for the Origins of Ultra-High-Energy Cosmic Rays (2024), https://arxiv.org/abs/2412.17201.
6. H. Salazar and L. Villaseñor, Rayos cósmicos ultraenergéticos: el Observatorio Pierre Auger, Ciencia *57* (2006) 64.
7. P. Carlson, Discovery of cosmic rays, *AIP Conference Proceedings* **1516** (2013) 9, https://doi.org/10.1063/1.4792532
8. J. Autran *et al*., Characterization of atmospheric muons at sea level using a cosmic ray telescope, *Nucl. Instrum. Methods Phys. Res. A.* **903** (2018) 77, https://doi.org/10.1016/j.nima.2018.06.038
9. T. K. Gaisser, Cosmic Rays and Particle Physics (Cambridge University Press, 1990).
10. S. Navas *et al*., Review of Particle Physics, *Phys. Rev. D* **110** (2024) 030001, https://doi.org/10.1103/PhysRevD.110.030001
11. ChipVerify, Verilog Tutorial, https://www.chipverify.com/verilog/verilog-tutorial (2023).
12. J. Serrano, Introduction to FPGA Design, https://cds.cern.ch/record/1100537/files/p231.pdf (2008).
13. L. H. Crockett *et al*., The ZYNQ book: embedded processing with the ARM Cortex-A9 on the Xilinx Zynq-7000 all programmable SoC (Strathclyde Academic Media, [S.l.], 2014), https://cds.cern.ch/record/2001018, The book can be consulted by contacting: DGS-RP-IL: Bellotta, Antonio.
14. L. Villaseñor, RedPitaya Hello World FPGA, https://github.com/lvillasen/RedPitaya-Hello-World-FPGA (2025),
15. L. Villaseñor, RedPitaya Muon Decay, https://github.com/lvillasen/RedPitaya-Muon-Decay (2025),
16. L. Villaseñor, Muon Decay Analysis, https://github.com/lvillasen/Muon-Decay (2025), Accessed: 2025-06-08.
17. J. Nocedal and S. J. Wright, Numerical Optimization, 2nd ed. (Springer New York, NY, 2006), https://doi.org/10.1007/978-0-387-40065-5